Hindawi
Adsorption Science & Technology
Volume 2022, Article ID 3137870, 13 pages
https://doi.org/10.1155/2022/3137870

Research Article

Adsorptive Removal of Alizarin Red S onto Sulfuric Acid-Modified Avocado Seeds: Kinetics, Equilibrium, and Thermodynamic Studies

G. Bharath Balji[1,2] **and P. Senthil Kumar**[1,2]

[1]*Department of Chemical Engineering, Sri Sivasubramaniya Nadar College of Engineering, Kalavakkam 603110, India*
[2]*Centre of Excellence in Water Research (CEWAR), Sri SivasubramaniyaNadar College of Engineering, Kalavakkam 603110, India*

Correspondence should be addressed to P. Senthil Kumar; senthilkumarp@ssn.edu.in

Received 13 September 2022; Revised 29 October 2022; Accepted 1 November 2022; Published 10 November 2022

Academic Editor: Muhammad Raziq Rahimi Kooh

The present work evaluates the synthesis of a novel, inexpensive, and environmentally friendly chemically-treated avocado seed powder (CTASP) as an adsorbent in removing alizarin red S (ARS) from synthetic solution. By using a set of analytical techniques, including FTIR, XRD, EDX, RS, and SEM, the adsorbent was characterized for its physical and chemical properties. Batch study experiments were conducted to determine the effectiveness of the CTASP as an adsorbent. The maximum adsorption capacity of 67.08 mgg^{-1} was attained at optimum conditions of 3 gL^{-1} adsorbent dosage, pH 3, contact time of 30 min, and at temperature 303 K. After 30 minutes, the equilibrium was reached, and the experimental data was explained for isotherm, kinetic, and thermodynamic processes. The results indicated that pseudo-second-order kinetics and the Freundlich isotherm were the best fits for the data. The findings of the analysis of the thermodynamic parameters for the process showed that the system was an exothermic and spontaneous. According to the desorption studies, 0.1 M NaOH can be utilized as a separating reagent to desorb 90.53% of ARS that was adsorbed. Regeneration experiments were conducted to make the process more practical and affordable, and it was discovered that the CTASP adsorbent could be successfully regenerated up to four times. In comparison with other adsorbents, the current low-cost adsorbent had the exceptional regenerative capability and delivered multilayer adsorption capacity. Additionally, it has been demonstrated that the CTASP is an effective material for the detoxification of ARS dye from wastewater.

1. Introduction

As the world's population grows, the demand for resources is to keep up with the rising level of living. Aside from an increase in demand for a variety of other commodities, people are very much interested in living in a Hi-Tech world, and they wanted to enjoy the benefits of science and technology. Besides, environmental pollution is inevitable but that can be controlled by different pollution-controlled techniques [1, 2]. Water pollution is one of the most damaging forms of pollution and is thought to have a critical role in environmental contamination. The effluents from industrial activities are considered to be the most significant source of water contamination, among many others. This effluent mainly contains a lot of organic matter, inorganic matter, heavy metals, and toxic dyes [3]. Incorporation of colors in different industrial activities induces the presence of the same in water resources, thereby contaminating the water bodies. Around half of the dye is released as waste in water during the dyeing process due to the inadequate level of fixation among dyes and the surface to be colored. Worldwide, over 10,000 tonnes of dyes are used annually, with 10 to 20% of those being colorants. Additionally, 100 tonnes of dyes are released into waterways annually, which is the main

contributor to water pollution. The level of BOD, COD, TDS, and TSS will increase proportionally as dyes become more accessible in the water. [1, 4].

In general, organic and inorganic dyes have a variety of consequences when discharged directly into waterways without any pretreatment. One of the major characteristics of dyes is it can expose color easily in the water due to the availability of chromophore compound in its structure [5]. Due to its stability, easy to synthesize, and color varieties, it is used particularly in textile industries [6]. The color in the water affects the aquatic system, damages the water bodies, collapses the entire food chain which is very toxic, and creates harmful effects to the human beings like carcinogenic and mutagenic effects [7–9]. Alizarin red S (ARS) is among the highest-risk dyes available, and it is widely employed as a coloring agent in a range of industries, including textile, cosmetics, and many others. ARS dye is chemically identified as 1,2-dihydroxy-9,10-anthraquinonesulfonic acid sodium salt. Alizarin carmine, Mordant Red-3, diamond red-W, and ARS water-soluble are some of the other names for this dye. It is an anthraquinone dye which is very difficult to treat and also widely used in many areas [10]. It is an orange powder with no odour; besides, ingestion or contact with this type can lead to some of the following health effects such as eye and skin irritation, respiratory damage, blood-related disease, air borne diseases, severe headache, and methemoglobinemia. As a result, it is now required that ARS dye-containing effluents can be treated before being released into an aquatic environments to limit environmental damage. ARS is a tough, long-lasting dye that is both mutagenic and carcinogenic [11–13].

A variety of physicochemical techniques like electrocoagulation, electrochemical oxidation, photocatalysis, electrochemical treatment, ozonation, membrane filtering, and adsorption have been utilized to treat dye-polluted water [14–18]. Applicability of these methods is minimized because of the excessive usage of chemicals, low efficiency, high cost, deposition of secondary pollutants, and high operational and maintenance costs [19, 20]. Even at very low concentrations, the availability of dyes might lead to reduce the aesthetic value of water [21]. Particularly, to treat the durable dye like ARS in the wastewater using those methods is dissatisfactory, due to the dye's stability and its complex structure of aromatic rings [22, 23]. Adsorption is a productive method for removing dyes from industrial effluents when compared to other methods. [24–27]. Sorption via physical or chemical processes can minimize energy requirements as well as the quantity and toxicity of the resulting waste sludge, resulting in reduced environmental impacts [28]. With respect to previous research, some of the adsorbents that are employed are biomass, activated carbon, multiwall carbon nanotubes, nanoparticles, graphene oxide, bio sorbents, and metal-organic framework [29–34].

Taking that into consideration, multiple studies have recently converged on the use of inexpensive and abundant precursors like waste biomass for activated carbon preparation [35]. Due to its well-developed pore structure, economic effectiveness, ease of availability, and high surface area [36], activated carbon is repeatedly applied and preferred material

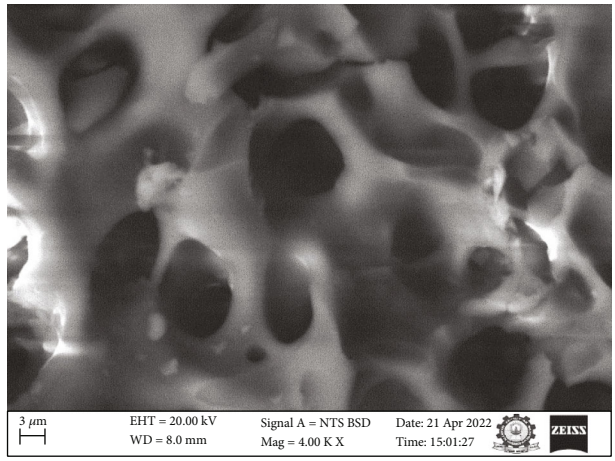

Figure 1: SEM image of CTASP before adsorption of dye.

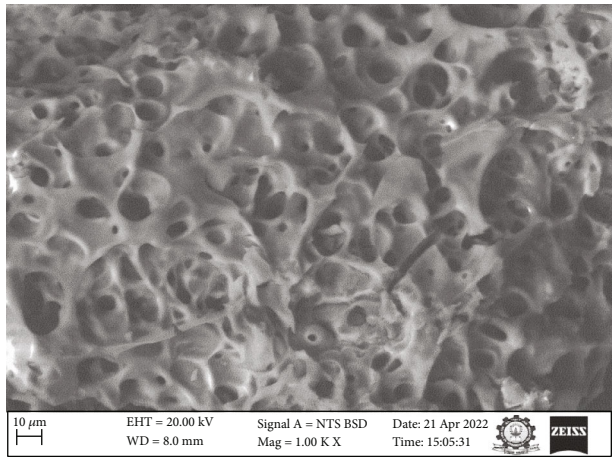

Figure 2: SEM image of CTASP after adsorption of dye.

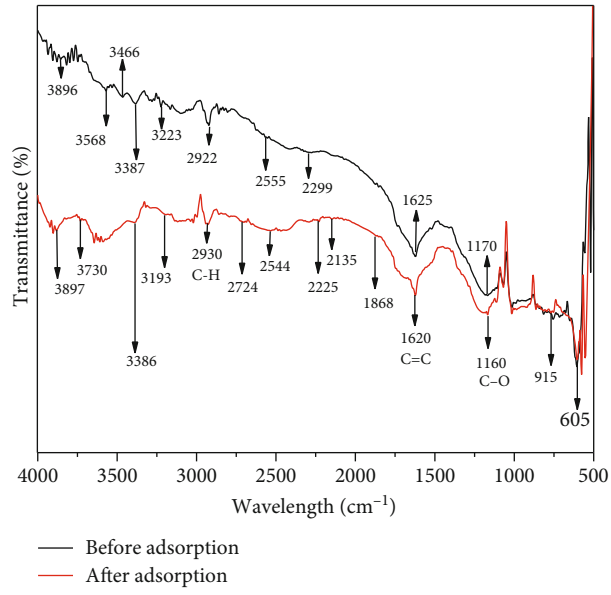

Figure 3: FTIR spectra of CTASP.

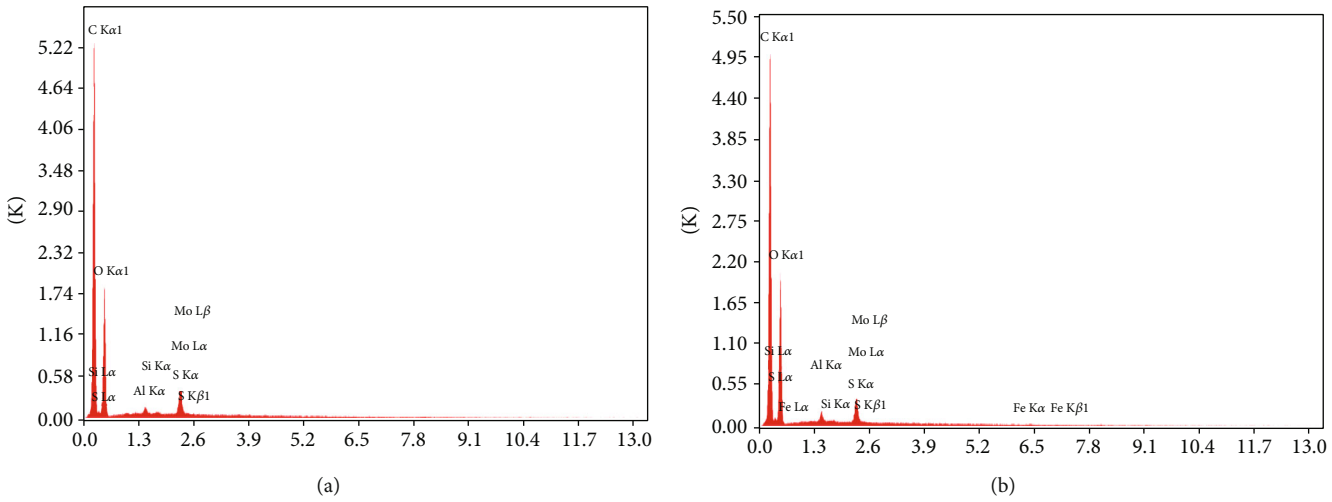

Figure 4: (a) EDS spectra of CTASP before adsorption of dye. (b) EDS spectra of CTASP after adsorption of dye.

Table 1: EDS spectra of ARS dye for before and after adsorption.

Elements	The weight percentage of CTASP	
	Before adsorption	After adsorption
Carbon (C)	58.2	56.2
Oxygen (O)	37.9	39.5
Aluminium (Al)	0.8	1.0
Silicon (Si)	0.2	0.3
Molybdenum(Mo)	2.2	1.7
Sulfur (S)	0.8	0.8
Iron (Fe)	—	0.4

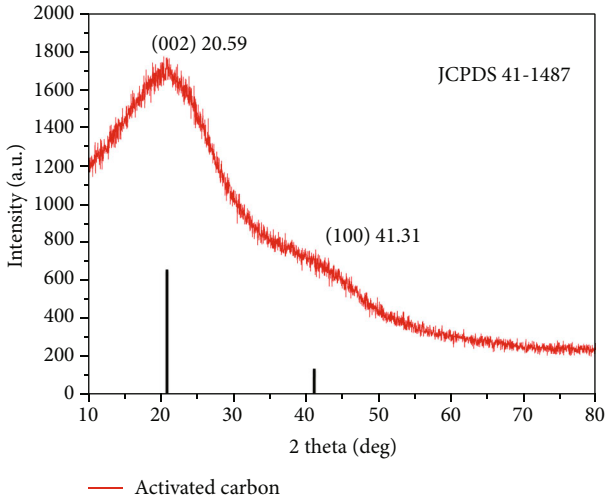

Figure 5: XRD of CTASP.

for the elimination of various hazardous dyes. In general, commercial-activated carbon is fairly expensive to produce, so it has stimulated the research interest in developing cost-effective, high-efficiency, and eco-friendly adsorbents through the use of several sources [37, 38].

The exploration of various adsorbent applications, such as the usage of avocado seeds, is necessary to get beyond all the constraints listed above. However, avocado seeds are a waste product that are typically thrown away without thinking about their possible use as an adsorbent. It is highly efficient, environmentally friendly, and economical adsorbent. The primary benefit of employing avocado seed as an adsorbent is turning waste into a material that may be used to address the emerging water pollution.

The main agenda of the research is to use the adsorption approach to reduce the elevated levels of ARS in water. As an adsorbent, chemically-treated avocado seed powder (CTASP) is used, which is not mentioned in any of the previous studies. Waste seeds were collected from nearby juice shops that was converted into activated carbon through a chemical method, which is utilized to eliminate ARS dye from water. Because seeds are not cast-off, the young plant's growth is unaffected. The proposed work offers a way to increase humanity's well-being. The article describes the adsorption capabilities of avocado seed that have been chemically treated. Batch adsorption is being investigated, to maximize efficiency by improving the regulating parameters. Because the adsorbent produced from avocado seed was a unique adsorbent in dye removal studies, it has undergone some basic modifications such as acid treatment. SEM, EDS, FTIR, RS, and XRD characterization experiments were carried out. Isotherms, kinetics, and thermodynamic models were also performed. The regeneration efficiency of the CTASP material was discussed in detail. The effectiveness of the CTASP adsorbent was compared to previous research works.

2. Experimental Section

2.1. Chemical Reagents Used. Chemicals of the analytical reagent grades were utilized in this experiment. To prepare the standard dye solution, ARS ($C_{14}H_7NaO_7S$) was purchased from Sisco Research Lab, India with analytical grade. Without any modification or additional purification, dyes were utilized. For the adsorbent's activation, sulfuric acid

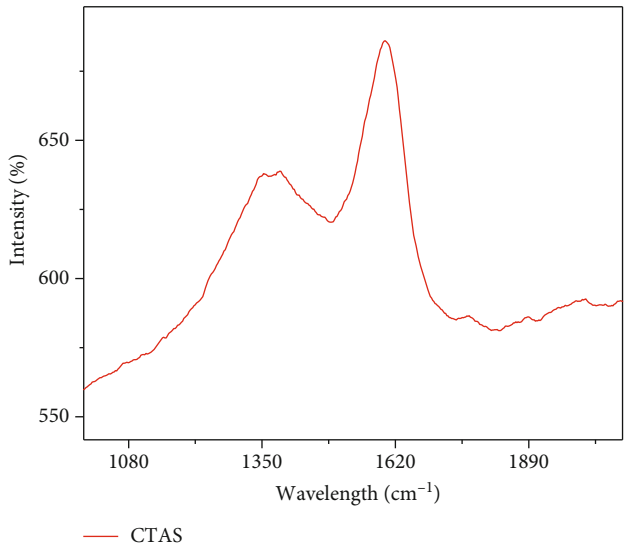

Figure 6: Raman Spectroscopy of CTASP.

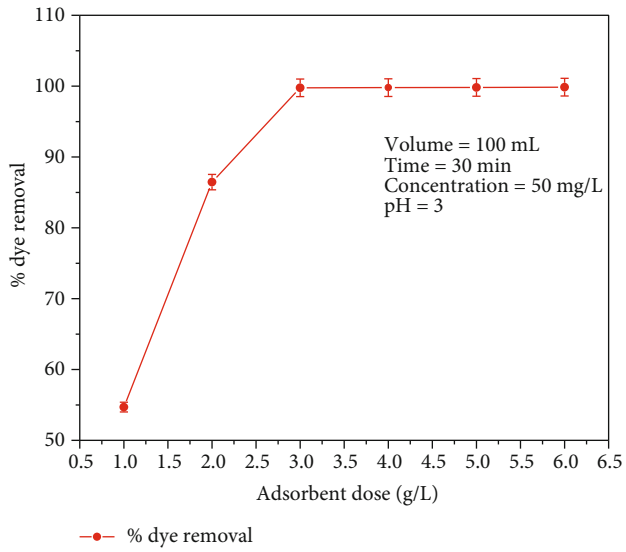

Figure 7: Percentage removal of ARS dye at various dose rates.

(H_2SO_4, 98%, Thermo Fisher Scientific India Pvt Ltd) were used in this study. Sodium hydroxide (NaOH, 97%, Merck Life Sciences Private Limited), hydrochloric acid (HCl, 37.0%, Thermo Fisher Scientific India PvtLtd). The stock solution of 1000 mg L^{-1} of ARS dye was synthesized by diluting 0.1 g of ARS dye in 100 mL of deionized water. Then, the required dye solutions of desired concentration, which is referred to as an adsorbate, were obtained through successive dilution.

2.2. Preparation and Characterization of Adsorbate. The avocado seeds were procured from a neighboring juice shop in Chennai, India. Then, it was then broken up into tiny pieces up to 4 mm, thoroughly washed with deionized water, sun-dried, and then dried in oven for 3 h at 100°C. The dried material was then carried inside and allowed to warm up. Then, it was labeled as chemically-treated avocado seed

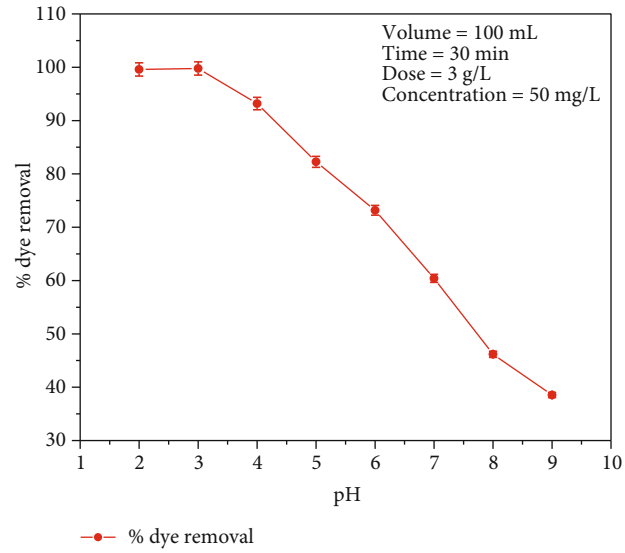

Figure 8: Effect of pH on ARS dye elimination.

powder after being impregnated with sulfuric acid in a 1 : 2 ratio (CTASP). Deionized water was used to remove the excess sulfuric acid by a series of washing up to the solution's pH became neutral. Then, the cleaned carbon samples were stored for later use in an airtight container after being dried at 110°C.

Using an EVO18 Scanning Electron Microscope (SEM), the morphological characteristics of the CTASP adsorbent were evaluated (Carl Zeiss). The magnification range was set to 2500 X and 5000 X, and a 20 kV acceleration voltage was used. Using the Quantax 200 and X Flash 6130 EDS analyzers, the composition of the adsorbents was studied along with the concentration of the available elements. Fourier transform infrared spectroscopy (FTIR) was used to identify the functional groups of CTASP on a Perkin Elmer e L1600300, Llantrisant, UK. Raman Spectroscopy analysis was performed to determine the presence of carbon compound in the wavelength of 532 nm with the power of 2 Mv and 30 s of exposure time using WelTec GmbH Germany, Alpha 300R model. A D8-advanced X-ray diffractometer (XRD) from Bruker (Germany) was used to determine the nature of the adsorbent. UV Spectrophotometer (Model: JASCO V-630) was used to assess the analytical measurement of dye.

2.3. Adsorption Experiments. Before adding CTASP to the adsorbate, the moisture content in the CTASP is eliminated using the hot air oven which was operated at 90°C for 2 h. Then, it was shaked in an orbital shaker for proper interaction at 140 rpm after adding the suitable quantity of CTASP to a conical flask containing ARS dye solution to accomplish the desired adsorption. Later, using No. 42 filter paper, the solid adsorbent was separated from the adsorbate. After that, a UV Spectrophotometer was used to evaluate the treated solution with residual dye concentration. By modifying the adsorption influencing parameters, studies on batch adsorption were conducted in the pH (2–9), shaking time (10–60) min, adsorbent dosage 1-6 g L^{-1}, initial dye concentration

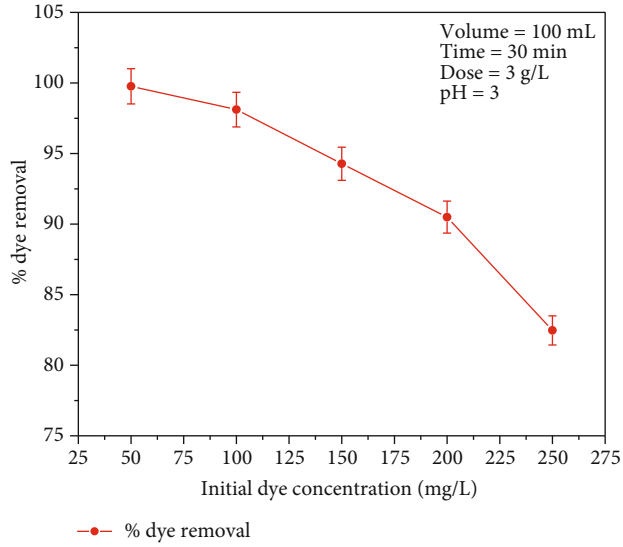

Figure 9: Removal of ARS dye at various initial concentrations.

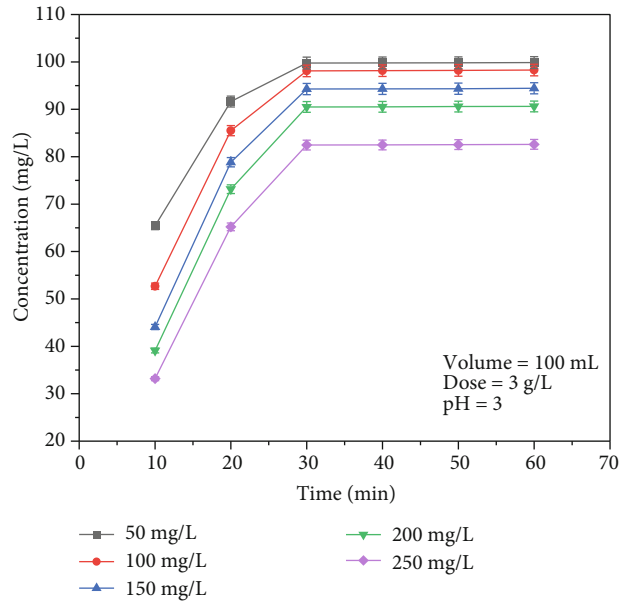

Figure 10: Effect of contact time on ARS dye removal.

(50-250) mg L^{-1}, and temperature ranges from 303 K to 333 K. The solution's pH was varied by using 0.1 N NaOH and 0.1 N HCl. To ensure consistent results, the entire sorption experiment was tripled. Measurement of dye concentration before and after adsorption is considered as C_o and C_e.

The adsorption efficiency of the process was determined by the following equation,

$$\%\text{Removal of ARS dye} = \frac{(C_o - C_e)}{C_o} \times 100. \quad (1)$$

The adsorption capacity was determined by the equation,

$$Q_e = \frac{(C_o - C_e)}{m} \times V, \quad (2)$$

where the terms C_o and C_e refer to the dye concentration levels before and after adsorption (mg L^{-1}), respectively. Here, Q_e stands for the CTASP's equilibrium adsorption capacity (mg g^{-1}), while V (L) and m (g) represent the volume and weight of ARS dye solution and CTASP adsorbent, respectively.

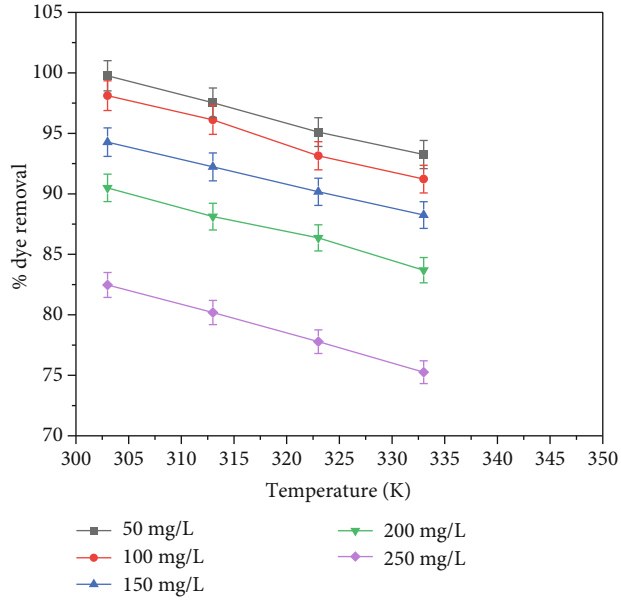

Figure 11: Effect of temperature on ARS dye removal.

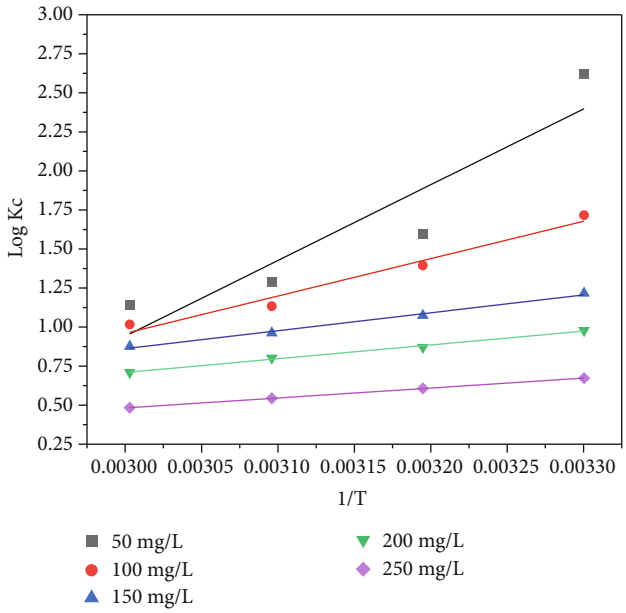

Figure 12: Thermodynamic analysis for the elimination of ARS dye by CTASP adsorbent.

Table 2: Thermodynamic parameters for the adsorption of ARS dye onto the CTASP.

Initial concentration of ARS dye (mg/L)	ΔH^o (kJ/Mol)	ΔS^o (J/Mol/K)	ΔG^o (kJ/Mol)			
			303	313	323	333
50	-92.854	-260.401	-15.211	-9.565	-7.969	-7.269
100	-45.80	-119.019	-9.954	-8.352	-7.008	-6.480
150	-21.977	-49.4379	-7.057	-6.438	-5.951	-5.582
200	-16.898	-37.1072	-5.676	-5.214	-4.955	-4.527
250	-12.189	-27.323	-3.900	-3.638	-3.364	-3.080

Table 3: Isotherm parameters.

Isotherm models	Parameters	Values
Langmuir	K_L (L/mg)	0.4791
	q_{max} (mg g^{-1})	67.08
	R^2	0.8643
	SSE	238.6
	RMSE	8.918
Freundlich	K_F (mg g^{-1}) (L mg^{-1})$^{1/n}$	28.47
	N	4.181
	R^2	0.9939
	SSE	10.73
	RMSE	1.891

3. Results and Discussion

3.1. SEM Analysis. Scanning Electron Microscope is a favourable instrument for assessing the surface morphology of the CTASP adsorbent. The available pores and cavities on the adsorbent's surface are one of the main reasons for the adsorption. Available pores at the adsorbent's surfaces will decide the effective elimination of ARS dye through adsorption. As seen in Figure 1, CTASP prior to adsorption, many active sites were produced as a result of chemical activation using sulfuric acid. The pores and cavities had a flaky, erratic structure. The ARS dyes were trapped in the pores of CTASP after adsorption, as shown in Figure 2, confirming the efficiency of the dye removal procedure. As a result, the amount of ARS dyes in the synthetic wastewater was diminished. The elimination of copper ions from wastewater by surface modified Delonix Regia seeds followed the same trend where sulfuric acid induced the adsorbent's surface area and pore density to increase [39].

3.2. FTIR Analysis. FTIR is utilized to look at the various chemical bonds that are present in the material. To determine its applicability, ACs synthesized from avocado seeds employing chemical treatment were used in the current investigation. Figure 3 displays the CTASP adsorbent sample taken for FTIR analysis. Broad stretching at 3387 cm^{-1} was seen in the FTIR analysis both before and after adsorption. These wide peaks were attributed to the O-H stretching vibration of hydroxyl groups linked to the structure or surface-adsorbed moisture, which conformed the existence of the hydroxyl group [40]. Sharp peaks shift at 1625-1620 cm^{-1} and 2922-2930 cm^{-1}and indicated the existence of C-O stretching in the aldehyde and ketone group and C-H stretching in the alkane group [41]. The existence of an amine group was suggested by the wider peaks at 1170 cm^{-1} and 1160 cm^{-1} for before and after adsorption, respectively [42]. Since it does not present in an isolated state with hydrogen, hydroxyl bonds play a significant role in the adsorption process. As a result, a stable structure was created [43].

3.3. EDS Analysis. In Figures 4(a), 4(b), and Table 1, EDS spectra of the CTASP adsorbent were shown both before and after the adsorption of ARS dye. The synthesized CTASP adsorbent can be seen in Table 1 which contains the components C, O, Al, Si, Mo, S, and Fe. Similar components were also shown in the after-adsorption of dyes. The existence of Si, which could be brought on by contaminants like dust and dirt, was confirmed by EDS, and the presence of aluminium was confirmed by the samples' coating at the time of examination. Additionally, the efficacy of the adsorption process was indicated by the elements in the dye's weight percentage of the CTASP dyes after-adsorption process. In the same way, after adsorption, the spectrum plots were shown in Figures 4(a) and 4(b), respectively.

3.4. XRD Analysis. Figure 5 shows the broad peaks of chemically-activated carbon, and there was no any well-defined diffraction peaks at 22° and 41.5°, portraying that the present carbon was amorphous. The peak at 41.5° was very weak, which suggested that the carbon structure was formed. The lack of distinct peaks revealed the structure's disordered nature and reflects the amorphous phase of carbon. This disordered carbon had a greater number of active sites and a high surface area, which facilitated the good adsorption. Because of the disordered carbons, CTASP had strong adsorption capacities [44, 45].

3.5. Raman Spectroscopy. The application of the Raman spectrum yields data on the molecular vibration and rotational energy for the specimen, which indicates the level of disorderliness of the structure. The samples possessed D and G bands that are attributed to the crystalline structure's instability and defection, as well as the carbon materials' graphitic nature as shown in Figure 6. The common spectra of carbon compounds have two notable peaks at about 1355 cm^{-1} (D band) and 1600 cm^{-1} (G band). The value of R (I_D/I_G) is used to define the degree of disordering in

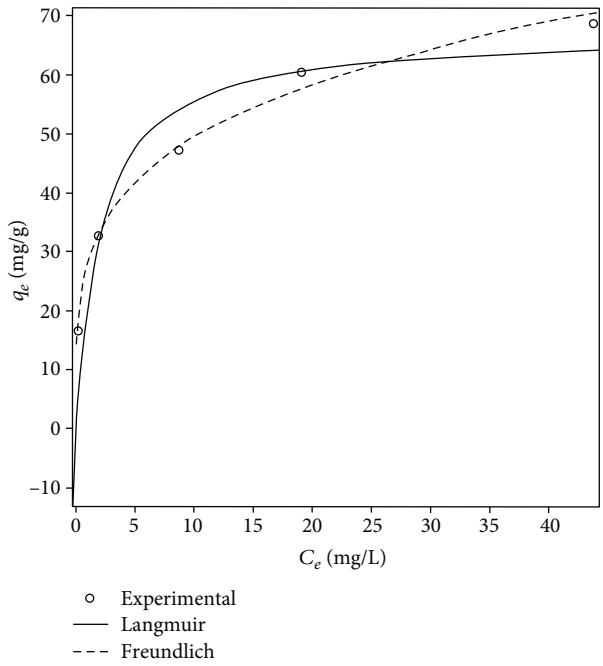

FIGURE 13: Isotherm study for the elimination of ARS dye by CTASP adsorbent.

carbon-based materials. ID and IG were determined for the integral intensities of D and G peaks of this spectrum [46, 47]. The same pattern of Raman spectra was also exhibited in the elimination of methylene blue dye by utilizing raw-activated carbon [48].

3.6. Effect of Adsorbent Dosage. On retaining the concentration of ARS dye, the pH of the adsorbate, and shaking time for the process (50 mg L^{-1}, 3 pH, and 30 min), the dosage of CTASP was varied from 1 to 6 g L^{-1}in a synthetic dye solution. From Figure 7, it was noticed that the effectiveness of the elimination of ARS dye was raised rapidly from 54.69% to 99.762%. The main reason for the improved efficacy was the increase in adsorbent dosage from 1-3 g L^{-1}. As the adsorbent dose rate increased, the adsorbent surface area also increased, and it leads to improved removal efficiency [49]. Beyond the dosage of 3 g L^{-1}, only very slight changes in the removal efficiency were observed, and it was noted. Once the equilibrium stage was achieved on the adsorbent surface, all the active sites were occupied by the dye molecules that there will not be any more adsorption. Thus, 3 g L^{-1} was an optimal adsorbent dose for the effective elimination of ARS dye in this process. The same trend of the result was noticed in eliminating this dye from synthetic effluent using a variety of chitosan as an effective adsorbent [50].

3.7. Effect of pH. ARS dye removal by CTASP was hugely affected by the pH effect. By maintaining the dosage of CTASP at 0.3 g in 100 mL, 50 mg L^{-1} of ARS dye concentration with the variation of pH from 2 to 9 for about 30 min. The alteration of pH with its percentage removal was shown in Figure 8. ARS dye contained a sulfonic acid group, which made it negatively charged in the liquid phase. So, a solid electrostatic force of attraction between the positively charged H^+ and negatively charged ARS takes place [51]. The maximum removal percentage of 99.76% for CTASP was achieved at pH 3. It was observed that the efficacy of dye elimination decreased as the pH rised to the alkali stage. The release of hydroxyl ions proceeds, when the basic pH was attained causing a repulsive force in the reaction. Electrostatic repulsion occurs between ARS dye and the OH- ions because of the negative charge of the dye. The same trend of the result was noticed in the existing study, where Nano-Fe_3O_4 and corn cover composite have been utilized as an adsorbent material for the successful elimination of ARS dye, with better removal efficiency occurring in the acidic pH range [52].

3.8. Effect of Initial Dye Concentration. To get a better understanding of the effective dye elimination process, the experimental study was executed by varying initial dye concentrations from 50, 100, 150, 200, and 250 mg $L^{-1}$with the guideline followed in section 3.7. Figure 9 showed the percentage removal of ARS dye concentration by CTASP adsorbent. The concentration ranged from 50 mg L^{-1} to 250 mg L^{-1} to assess the adsorbent's effectiveness under different dye concentrations. When the initial concentration of ARS dye raised, the removal efficiency declined. The same adsorbent dose was used at different initial dye concentrations for adsorption studies. This indicates that the active sites on the adsorbent surface were constant. When the initial dye concentration was increased, then the ratio of available free dye molecules to the active sites was increased which results in the reduction of removal of dye molecules from water system. The constant active sites of the adsorbent were able to remove the fixed number of dye molecules even though it was operated under different initial dye concentrations. The produced adsorbent was able to work for the dye concentration of 50 to 250 mg L^{-1}.

3.9. Effect of Contact Time. One of the key influencing factors in adsorption analyses is contact time. Effects of contact time on the efficacy of ARS dye removal by CTASP were depicted in Figure 10. The shaking time was altered from 10 to 60 min. The initial dye concentrations of the adsorbate were 50, 100, 150, 200, and 250 mg L^{-1}; the dosage of CTASP is 3 g L^{-1}, and the pH was set to be 3, accordingly. When utilizing CTASP, the elimination process occured more quickly for the first 30 min, and beyond 30 min, there was only a slight change in the percentage removal. The majority of the active sites get saturated, and few would be left. Over time, there were fewer active sites available, decreasing the probability of dyes adhering to the adsorbent surface. For CTASP, saturation was attained within 30 minutes of the contact period. To further understand the mechanism, the data was employed for kinetic analysis. The same pattern of the result wasa achieved in the removal of ARS dye by phenyl/amine end-capped tetra aniline [53].

3.10. Effect of Temperature. Figure 11 illustrates temperature effects on adsorption efficiency of the ARS dye by CTASP

Table 4: Comparison of CTASP's adsorption capability with already available adsorbents.

Adsorbent	Adsorption capacity ($mg\,g^{-1}$)	Reference
Single-walled carbon nanotubes (SWCNT)	312.5	Machado et al., [62]
Fe3O4@NiO, core–shell magnetic nanoparticle	223.30	Nodehi et al., [63]
Multiwalled carbon nanotubes (MWCNT)	135.2	Machado et al., [62]
Activated carbon incorporated with gold nanoparticles	123.4	Roosta and Ghaedi, [64]
Polymer resin and waste cotton fibers	104	Wanassi et al., [65]
Iron nanoadsorbents from mixed waste biomass	42.58	Gautam et al., [66]
Spirulinaplatensis biomass	17.15	Nasoudari et al., [67]
Acid-treated avocado seed powder	**67.08**	This study

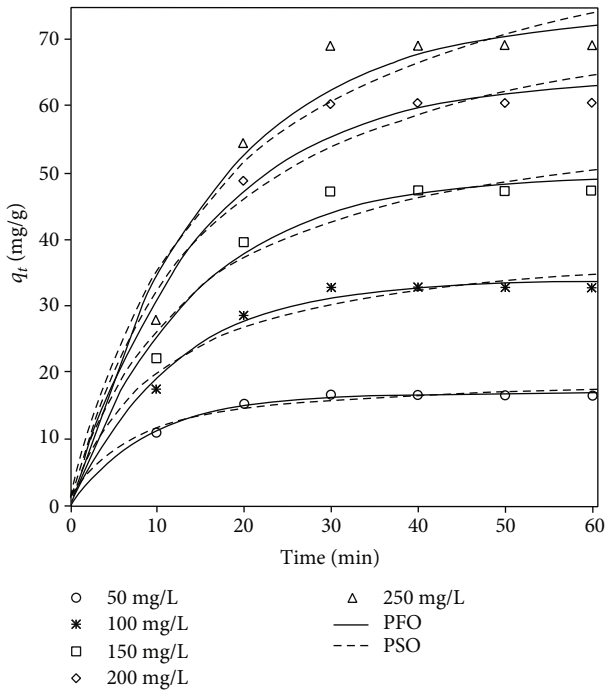

Figure 14: Kinetic study for the elimination of ARS dye by CTASP adsorbent.

adsorbent. With a rise in adsorbate temperature, ARS dye removal effectiveness reduced. The processes are also controlled by other experimental parameters such as a dosage of $3\,g\,L^{-1}$, adsorbate pH 3, shaking time of 30 min, and dye concentrations varied from $50\,mg\,L^{-1}$ to $250\,mg\,L^{-1}$ with temperatures between 303 and 333 K. The exothermic nature of the adsorption process was evidenced by the decrease in the uptake of ARS dye by CTASP adsorbent. This may be due to ARS molecules tend to migrate from the adsorbent's interface to the aqueous medium as the temperature increased [54]. The increased solubility of the dye when the temperature was raised thought to be the cause of the CTASP's reduced adsorption capability at high temperatures. Additionally, desorption of the dye molecules from the activated carbon via a weakening of the electrostatic force of attraction was possible also at high temperatures [55]. Therefore, lower temperatures were thought to be preferable for the CTASP dye removal process. Similar outcomes in the elimination of ARS dye by organically-modified micron-sized vermiculite were obtained [56].

Studies on thermodynamics assist in identifying the nature of the process that take place during adsorption and the process's spontaneity were performed. This study was used to access the favorable nature of the process. Using CTASP as an adsorbent, the adsorbate concentration varied from 50 to $250\,mg\,L^{-1}$, and the adsorption of the ARS dye was examined at different temperatures between 303 and 333 K. The following equations were used to estimate the values of ΔG^o, ΔH^o, and ΔS^o.

The thermodynamic parameters, such as ΔH^o and ΔS^o, were derived from Figure 12, and ΔG was obtained using the formula. Table 2 contains a list of the thermodynamic study's parameters. The fact that ΔG values are negative indicated that conditions were favorable for both spontaneous reactions and the adsorption process. The exothermic nature of the dye adsorption was represented by the negative values of ΔH^o. The negative values of ΔS^o indicate the decrease in the randomness of the adsorption process.

$$
\begin{aligned}
Kc &= \frac{C_{Ae}}{C_e},\\
\Delta G^{o} &= -\mathrm{RT}\ln Kc,\\
\Delta G^o &= \Delta H^o - T\Delta S^o,\\
\ln \mathrm{Kc} &= -\frac{\Delta H^o}{\mathrm{RT}} + \frac{\Delta S^o}{R},\\
\log \mathrm{Kc} &= -\frac{\Delta H^o}{2.303\mathrm{RT}} + \frac{\Delta S^o}{2.303R}.
\end{aligned}
\tag{3}
$$

3.11. Adsorption Isotherms. The adsorption efficiency and the governing mechanism can be roughly estimated using the isotherm experiments for the removal ARS dye by CTASP adsorbent. It explains the interactions between an adsorbent and an adsorbate molecule to achieve equilibrium.

The Langmuir model [57] assumes that the sorbent surface is homogeneous and has a finite number of sites with a

Table 5: Rate constants and other parameters for the adsorption kinetics.

Models	Parameters	Values				
		50 mg/L	100 mg/L	150 mg/L	200 mg/L	250 mg/L
	q_e, exp (mg/g)	17.15	32.92	47.53	60.86	68.95
PFO	k_1 (min^{-1})	0.1091	0.08358	0.0722	0.06646	0.06241
	$q_{e,\ cal}$ (mg/g)	16.88	33.85	49.55	64.08	73.7
	R^2	0.9845	0.9604	0.9434	0.9359	0.9275
	SSE	0.4078	7.334	28.97	61.52	100.4
	RMSE	0.3193	1.354	2.691	3.922	5.011
PSO	k_2 (g/mg.Min)	0.00816	0.002414	0.001241	0.0008203	0.0006321
	$q_{e,\ cal}$ (mg/g)	19.15	40.46	61.26	80.82	94.48
	R^2	0.9063	0.8943	0.886	0.8843	0.8797
	SSE	2.465	19.59	58.32	111	166.6
	RMSE	0.785	2.213	3.818	5.269	6.454
Intraparticle diffusion	k_p (mg/(g.$min^{(1/2)}$))	1.127	3.0413	5.098	7.043	8.491
	C	9.0173	12.133	12.584	12.511	11.036
	R^2	0.6229	0.6512	0.668	0.683	0.69

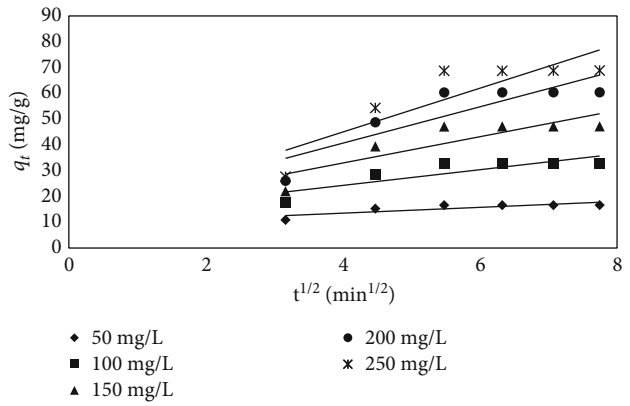

Figure 15: Intraparticle diffusion.

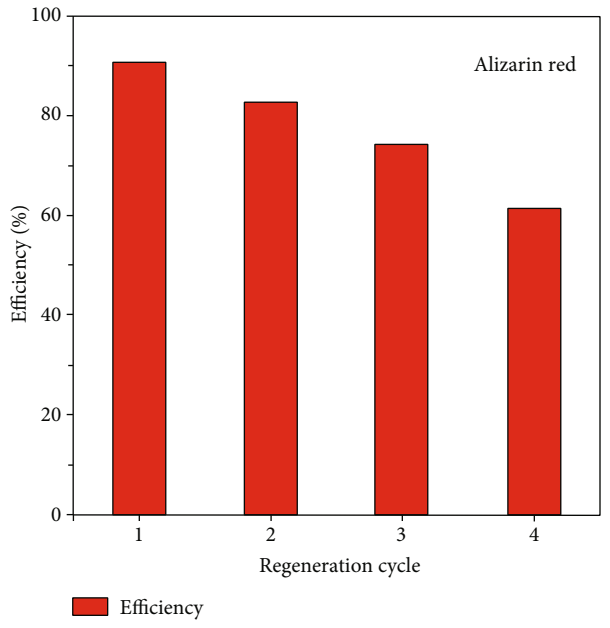

Figure 16: Regeneration of CTASP adsorbent.

monolayer. It is expressed mathematically as follows.

$$q_e = \frac{q_m K_L C_e}{1 + K_L C_e}, \quad (4)$$

where C_e is equilibrium concentration of ARS dye in an aqueous medium (mg L^{-1}), q_m is maximum monolayer adsorption capacity (mg g^{-1}), q_e is amount of adsorbate adsorbed at equilibrium condition (mg g^{-1}), and K_L is Langmuir constant (L/mg).

The adsorption equilibrium was first described by Freundlich, an experimental equation that relied on the observation that adsorption takes place on a miscellaneous surface with numerous layers. Enthalpy of the adsorption mechanism reduced rapidly with the occupation of the active sites. The following equation can be used to express the Freundlich isotherm [58]:

$$qe = K_F C_e^{1/n}, \quad (5)$$

where K_F ((mg g^{-1}) (L $mg^{-1})^{1/n}$) stands for the Freundlich constant, which is used to evaluate the degree of adsorption. Where n is the Freundlich coefficient used to assess the strength of the adsorption. The adsorbent surface is more heterogeneous as the Freundlich slope value tends to zero. The computed values and associated R^2 of the Langmuir and Freundlich isotherms were shown in Table 3. The obtained R^2 values were used to assess the quality of the proposed models. As Freundlich had a higher R^2 value than Langmuir, Figure 13 and Table 3 indicate that Freundlich was a better fit. The Freundlich model could be utilized to derive the formation of a multilayer surface on the adsorbent. CTASP had a maximum adsorption capacity of

67.08 mg g^{-1}. Here, it is reasonable to suggest that the Freundlich isotherm governs the adsorption of the ARS dye by the CTASP adsorbent.

A comparison of CTASP's adsorption capability with already available adsorbents was listed in Table 4. The results showed that the CTASP has a good adsorption potential for the removal of ARS dye from water.

3.12. Adsorption Kinetics. Kinetic models are applied to interpret the adsorption process and its reaction pathways. It improves clarity in designing a treatment system. In this study, Pseudo-first-order (PFO) [59], Pseudo-second-order (PSO) [60], and intraparticle diffusion (IPD) models are evaluated to understand the reaction mechanism of CTASP adsorbent. The following are the kinetic models,

$$q_t = q_e(1 - \exp(-k_1 t)),$$
$$q_t = \frac{q_e^2 k_2 t}{1 + q_e k_2 t}. \quad (6)$$

The kinetic data was applied to the kinetic models (Figure 14), and the predicted results were available in Table 5. The results observed that the PSO had higher correlation coefficients (R^2) and low error (SSE and RMSE) values than the PFO kinetics. The fact that estimated and experimental results showed that the ARS dye exhibited an affinity for the CTASP adsorbent in the PSO kinetics. The adsorption process may be controlled by diffusion mechanism. At first, the dye molecules will migrate into the adsorbent surface from the bulk solution. These dye molecules would further diffuse into the interior part of adsorbent pore. Adsorption tooks place at the pore end of the adsorbent, where the intra particle diffusion happened at the interior pores of the adsorbent. The intraparticle diffusion model was given as follows [61]:

$$q_t = k_p t^{1/2} + C. \quad (7)$$

The rate-determining phase is significant in determining the process's mechanism (Figure 15). The coefficient of determination (R^2) value being as close to one as possible was selected as the best fit.

3.13. Regeneration Studies. The regeneration of the adsorbent material is necessary for any adsorption technique since regeneration influences the adsorbent's commercial feasibility [38]. Desorption analyses on the used CTASP were carried out to comprehend the CTASP's capacity for regeneration. The removal effectiveness of the regenerated activated carbon was evaluated using regeneration phases up to the fourth cycle (RAC). The adsorbent was first saturated by stirring 0.1 g of CTASP with 50 mL of a 200 mg L^{-1} ARS dye solution for 1 day. Then 0.1 M NaOH solution was agitated for 3 hours to desorb the saturated CTASP. After filtering, washing with deionized water and oven drying at 120°C were done. Then, it was used once more to remove the dye. This regenerated activated carbon was found to have a removal efficiency of 90.53%. Up to the fourth cycle, the adsorption and desorption were examined to analyze the efficiency of the regeneration cycle. The findings were shown in Figure 16 and showed that the reusability of the adsorbent up to the fourth cycle effectively and the adsorption efficiency of CTASP decreased to 61.43% from 90.53% in the first cycle. The reduction in efficiency might be due to blockage of active sites or loss of efficiency in removal of target pollutant.

4. Conclusion

This study evaluated the synthesis of a novel, inexpensive, and environmentally friendly chemically-treated avocado seed powder (CTASP) as an adsorbent. Then, it was utilized to eliminate the ARS dye in the synthetic effluent. Utilizing a set of techniques, including FTIR, XRD, EDX, Raman Spectroscopy, and SEM, the adsorbent was characterized. The experiments with altered pH values revealed that the solution's pH had a significant impact on the adsorption system for the adsorbate. A pH range of 3 was found to be suitable for the elimination of ARS dye. The active sites and the adsorbents surface area were increased when the dosage of the adsorbent increased, which in turn caused an increase in the efficiency of the ARS dye. CTASP was loaded to its maximum capacity with ARS dye at a dosage of 3 g L^{-1}.The better removal efficiency for ARS dye was achieved at 50 mg L^{-1} for the contact time of 30 min at a temperature of 303 K. The adsorbent's maximum adsorption capacity was reported to be 67.08 mgg^{-1}. The rate kinetics for the adsorption of ARS dye were best suited by the PSO following Freundlich isotherm. The exothermic nature of adsorption was experienced in thermodynamic studies, and it was proven by the fact that it became less spontaneous as temperature increased. The regeneration studies showed that the adsorbent can be utilized for up to four cycles with improved efficiency.

Data Availability

All data are available on request.

Conflicts of Interest

The authors declare that they have no conflicts of interest.

References

[1] M. I. Khamis, T. H. Ibrahim, F. H. Jumean, Z. A. Sara, and B. A. Atallah, "Cyclic sequential removal of alizarin red S dye and Cr (VI) ions using wool as a low-cost adsorbent," *Processes*, vol. 8, no. 5, p. 556, 2020.

[2] M. Muniyandi, P. Govindaraj, and G. B. Balji, "Potential removal of methylene blue dye from synthetic textile effluent using activated carbon derived from Palmyra (palm) shell," *Materials Today*, vol. 47, no. 1, pp. 299–311, 2021.

[3] K. Ikram, N. Jamila, M. Salman, M. Shehrbano, and A. Siddique, "Use of Polyalthia longifolia based alumina composites for the removal of reactive dyes from aqueous medium," *Desalination and Water Treatment*, vol. 185, pp. 364–374, 2020.

[4] M. Akram, M. Salman, U. Farooq et al., "Phthalate-functionalized Sorghum bicolor L.; an effective biosorbent for the removal of alizarin red S and bromophenol blue dyes from simulated wastewater," *Desalination and Water Treatment*, vol. 190, pp. 383–392, 2020.

[5] B. Lellis, C. Z. Fávaro-Polonio, J. A. Pamphile, and J. C. Polonio, "Effects of textile dyes on health and the environment and bioremediation potential of living organisms," *Biotechnology Research and Innovation*, vol. 3, no. 2, pp. 275–290, 2019.

[6] C. Osagie, A. Othmani, S. Ghosh, A. Malloum, Z. K. Esfahani, and S. Ahmadi, "Dyes adsorption from aqueous media through the nanotechnology: a review," *Journal of Materials Research and Technology*, vol. 14, pp. 2195–2218, 2021.

[7] M. M. Hassan and C. M. Carr, "A critical review on recent advancements of the removal of reactive dyes from dyehouse effluent by ion-exchange adsorbents," *Chemosphere*, vol. 209, no. 1, pp. 201–219, 2018.

[8] C. Ling, Z. Wang, Y. Ni, Z. Zhu, Z. Cheng, and R. Liu, "Superior adsorption of methyl blue on magneticNi–Mg–Coferrites: adsorption electrochemical properties and adsorption characteristics," *Environmental Progress & Sustainable Energy*, vol. 41, no. 6, article e13923, 2022.

[9] S. Zhang, S. Xu, Y. Ni, Z. Zhu, C. Ling, and R. Liu, "Adsorption mechanism and electrochemical characteristic of methyl blue onto calcium ferrite nanosheets," *Adsorption Science & Technology*, vol. 2022, article 6999213, 9 pages, 2022.

[10] F. Fu, Z. Gao, L. Gao, and D. Li, "Effective adsorption of anionic dye, alizarin red S, from aqueous solutions on activated clay modified by iron oxide," *Industrial & Engineering Chemistry Research*, vol. 50, no. 16, pp. 9712–9717, 2011.

[11] L. A. Adnan, P. Sathishkumar, A. R. M. Yusoff, T. Hadibarata, and F. Ameen, "Rapid bioremediation of alizarin red S and Quinizarine green SS dyes using *Trichoderma lixii* F21 mediated by biosorption and enzymatic processes," *Bioprocess and Biosystems Engineering*, vol. 40, no. 1, pp. 85–97, 2017.

[12] R. Rehman and T. Mahmud, "Sorptive elimination of alizarin red-S dye from water using *Citrullus lanatus* peels in environmentally benign way along with equilibrium data modeling," *Asian Journal of Chemistry*, vol. 25, no. 10, pp. 5351–5356, 2013.

[13] S. Venkatesh and V. Arutchelvan, "Biosorption of alizarin red dye onto immobilized biomass of *Canna indica*: isotherm, kinetics, and thermodynamic studies," *Desalination and Water Treatment*, vol. 196, pp. 409–421, 2020.

[14] B. Dadpou and D. Nematollahi, "Electrochemical oxidation of Alizarin Red-S on glassy carbon electrode: mechanistic study, surface adsorption and preferential surface orientation," *Journal of The Electrochemical Society*, vol. 163, no. 7, pp. H559–H565, 2016.

[15] P. K. Gautam, R. K. Gautam, S. Banerjee, M. C. Chattopadhyaya, and J. D. Pandey, "Adsorptive removal of alizarin red S by a novel biosorbent of an invasive weed *Mikania* micrantha," *National Academy Science Letters*, vol. 40, no. 2, pp. 113–116, 2017.

[16] B. Kamarehie, A. Jafari, M. Ghaderpoori, M. A. Karami, K. Mousavi, and A. Ghaderpoury, "Catalytic ozonation process using PAC/γ-Fe_2O_3 to alizarin red S degradation from aqueous solutions: a batch study," *Chemical Engineering Communications.*, vol. 206, no. 7, 2019.

[17] S. S. Ma and Y. G. Zhang, "Electrolytic removal of alizarin red S by Fe/Al composite hydrogel electrode for electrocoagulation toward a new wastewater treatment," *Environmental Science and Pollution Research,*, vol. 23, no. 22, pp. 22771–22782, 2016.

[18] F. Yi and S. Chen, "Electrochemical treatment of alizarin red S dye wastewater using an activated carbon fiber as anode material," *Journal of Porous Materials*, vol. 15, no. 5, pp. 565–569, 2008.

[19] A. B. Albadarin and C. Mangwandi, "Mechanisms of alizarin red S and methylene blue biosorption onto olive stone by-product: isotherm study in single and binary systems," *Journal of Environmental Management*, vol. 164, pp. 86–93, 2015.

[20] R. K. Gautam, P. K. Gautam, M. C. Chattopadhyaya, and J. D. Pandey, "Adsorption of alizarin red S onto biosorbent of *Lantana camara*: kinetic, equilibrium modeling and thermodynamic studies," *Proceedings of the National Academy of Sciences, India Section A: Physical Sciences*, vol. 84, no. 4, pp. 495–504, 2014.

[21] O. S. Ayanda, O. S. Amodu, H. Adubiaro et al., "Effectiveness of termite hill as an economic adsorbent for the adsorption of alizarin red dye," *Journal of Water Reuse and Desalination*, vol. 9, no. 1, pp. 83–93, 2019.

[22] D. Bhatia, N. R. Sharma, J. Singh, and R. S. Kanwar, "Biological methods for textile dye removal from wastewater: a review," *Critical Reviews in Environmental Science and Technology*, vol. 47, no. 19, pp. 1836–1876, 2017.

[23] R. Rehman, A. Raza, W. Noor, A. Batool, and H. Maryem, "Photocatalytic degradation of alizarin red S, amaranth, Congo red, and rhodamine B dyes using UV light modified reactor and ZnO, TiO_2, and SnO_2 as catalyst," *Journal of Chemistry*, vol. 2021, Article ID 6655070, 9 pages, 2021.

[24] M. Bagtash and J. Zolgharnein, "Hybrid central composite design for simultaneous optimization of removal of methylene blue and alizarin red S from aqueous solutions using *Vitis* tree leaves," *Journal of Chemometrics*, vol. 32, no. 2, pp. 1–13, 2018.

[25] P. S. Kumar, C. Senthamarai, and A. Durgadevi, "Adsorption kinetics, mechanism, isotherm, and thermodynamic analysis of copper ions onto the surface modified agricultural waste," *Environmental Progress & Sustainable Energy*, vol. 33, no. 1, 2014.

[26] T. Saeed, A. Naeem, I. U. Din et al., "Synthesis of chitosan composite of metal-organic framework for the adsorption of dyes; kinetic and thermodynamic approach," *Journal of Hazardous Materials*, vol. 427, article 127902, 2022.

[27] S. Samiee, F. Moosavi, and E. K. Goharshadi, "Adsorption of an azo dye graphene nanosheet: a molecular dynamics simulation study," *Physical Chemistry Research*, vol. 11, no. 1, pp. 117–127, 2023.

[28] B. Ramavandi, A. A. Najafpoor, H. Alidadi, and Z. Bonyadi, "ARS removal from aqueous solutions using Saccharomyces cerevisiae: kinetic and equilibrium study," *Desalination and Water Treatment*, vol. 144, pp. 286–291, 2019.

[29] G. R. Delpiano, D. Tocco, L. Medda, E. Magner, and A. Salis, "Adsorption of malachite green and alizarin red S dyes using Fe-BTC metal organic framework as adsorbent," *International Journal of Molecular Sciences*, vol. 22, no. 2, p. 788, 2021.

[30] R. K. Gautam, A. Mudhoo, and M. C. Chattopadhyaya, "Kinetic, equilibrium, thermodynamic studies and spectroscopic analysis of alizarin red S removal by mustard husk," *Journal of Environmental Chemical Engineering*, vol. 1, no. 4, pp. 1283–1291, 2013.

[31] M. Ghaedi, A. Hassanzadeh, and S. N. Kokhdan, "Multiwalled carbon nanotubes as adsorbents for the kinetic and

equilibrium study of the removal of alizarin red S and morin," *Journal of Chemical & Engineering Data*, vol. 56, no. 5, pp. 2511–2520, 2011.

[32] M. Ghaedi, A. Najibi, H. Hossainian, A. Shokrollahi, and M. Soylak, "Kinetic and equilibrium study of alizarin red S removal by activated carbon," *Toxicological and Environmental Chemistry*, vol. 94, no. 1, pp. 40–48, 2012.

[33] M. B. Gholivand, Y. Yamini, M. Dayeni, S. Seidi, and E. Tahmasebi, "Adsorptive removal of alizarin red-S and alizarin yellow GG from aqueous solutions using polypyrrole-coated magnetic nanoparticles," *Journal of Environmental Chemical Engineering*, vol. 3, no. 1, pp. 529–540, 2015.

[34] M. Liu, X. Zhang, Z. Li, L. Qu, and H. Runping, "Fabrication of zirconium (IV)-loaded chitosan/Fe_3O_4/graphene oxide for efficient removal of alizarin red from aqueous solution," *Carbohydrate Polymers*, vol. 248, p. 116792, 2020.

[35] P. C. Bhomick, A. Supong, M. Baruah, C. Pongener, C. Gogoi, and D. Sinha, "Alizarin red S adsorption onto biomass-based activated carbon:optimization of adsorption process parameters using Taguchi experimental design," *International journal of Environmental Science and Technology*, vol. 17, no. 2, pp. 1137–1148, 2020.

[36] H. Wang, Z. Li, S. Yahyaoui et al., "Effective adsorption of dyes on an activated carbon prepared from carboxymethyl cellulose: experiments, characterization and advanced modelling," *Chemical Engineering Journal*, vol. 417, article 128116, 2021.

[37] M. Baruah, A. Supong, P. C. Bhomick, R. Karmaker, C. Pongener, and D. Sinha, "Batch sorption–photodegradation of alizarin red S using synthesized TiO_2/activated carbon nanocomposite: an experimental study and computer modelling," *Nanotechnology for Environmental Engineering*, vol. 5, no. 1, 2020.

[38] P. C. Bhomick, A. Supong, M. Baruah, C. Pongener, and D. Sinha, "Pine cone biomass as an efficient precursor for the synthesis of activated biocarbon for adsorption of anionic dye from aqueous solution: isotherm, kinetic, thermodynamic and regeneration studies," *Sustainable Chemistry and Pharmacy*, vol. 10, pp. 41–49, 2018.

[39] A. Saravanan, T. R. Sundararaman, S. Jeevanantham, S. Karishma, P. Senthil Kumar, and P. R. Yaashikaa, "Effective adsorption of Cu(II) ions on sustainable adsorbent derived from mixed biomass (*Aspergillus campestris* and agro waste): optimization, isotherm and kinetics study," *Groundwater for Sustainable Development*, vol. 11, article 100460, 2020.

[40] N. Ali, F. Ali, I. Ullah et al., "Organically modified micron-sized vermiculite and silica for efficient removal of Alizarin Red S dye pollutant from aqueous solution," *Environmental Technology & Innovation*, vol. 19, article 101001, 2020.

[41] S. Benkaddour, R. Slimani, H. Hiyane et al., "Removal of reactive yellow 145 by adsorption onto treated watermelon seeds: kinetic and isotherm studies," *Sustainable Chemistry and Pharmacy*, vol. 10, pp. 16–21, 2018.

[42] S. Manna, P. Saha, D. Roy, B. Adhikari, and P. Das, "Fixed bed column study for water defluoridation using neem oil-phenolic resin treated plant bio-sorbent," *Journal of Environmental Management*, vol. 212, pp. 424–432, 2018.

[43] D. E. Jayashree, P. S. Kumar, P. T. Ngueagni, D. V. N. Vo, and K. W. Chew, "Effective removal of excessive fluoride from aqueous environment using activated pods of *Bauhinia variegata* : Batch and dynamic analysis," *Environmental Pollution*, vol. 272, article 115969, 2021.

[44] S. J. Rajasekaran and V. Raghavan, "Facile synthesis of activated carbon derived from *Eucalyptus globulus* seed as efficient electrode material for supercapacitors," *Diamond and Related Materials*, vol. 109, article 108038, 2020.

[45] J. Rashid, F. Tehreem, A. Rehman, and R. Kumar, "Synthesis using natural functionalization of activated carbon from pumpkin peels for decolourization of aqueous methylene blue," *Science of the Total Environment*, vol. 671, pp. 369–376, 2019.

[46] K. Judai, N. Iguchi, and Y. Hatakeyama, "Low-temperature production of genuinely amorphous carbon from highly reactive nanoacetylide precursors," *Journal of Chemistry*, vol. 2016, Article ID 7840687, 6 pages, 2016.

[47] A. Rosenkranz, L. Freeman, B. Suen, Y. Fainman, and F. E. Talke, "Tip-enhanced Raman spectroscopy studies on amorphous carbon films and carbon overcoats in commercial hard disk drives," *Tribology Letters*, vol. 66, no. 2, p. 54, 2018.

[48] S. Cheng, L. Zhang, H. Xia, and J. Peng, "Characterization and adsorption properties of La and Fe modified activated carbon for dye wastewater treatment," *Green Processing and Synthesis*, vol. 6, no. 5, pp. 487–498, 2017.

[49] F. Banisheykholeslami, M. Hosseini, and G. N. Darzi, "Design of PAMAM grafted chitosan dendrimersbiosorbent for removal of anionic dyes: adsorption isotherms, kinetics and thermodynamics studies," *International Journal of Biological Macromolecules*, vol. 177, pp. 306–316, 2021.

[50] M. A. Khapre and R. M. Jugade, "Hierarchical approach towards adsorptive removal of alizarin red S dye using native chitosan and its successively modified versions," *Water Science and Technology*, vol. 82, no. 4, pp. 715–731, 2020.

[51] Z. Zhang, H. Chen, W. Wu, W. Pang, and G. Yan, "Efficient removal of alizarin red S from aqueous solution by polyethyleneimine functionalized magnetic carbon nanotubes," *Bioresource technology*, vol. 293, article 122100, 2019.

[52] J. Zolgharnein, Z. Choghaei, M. Bagtash, S. H. Feshki, M. Rastgordani, and P. Zolgharnein, "Nano-Fe_3O_4 and corn cover composite for removal of alizarin red S from aqueous solution: characterization and optimization investigations," *Desalination and Water Treatment*, vol. 57, pp. 27672–27685, 2016.

[53] Y. Liu, J. Li, J. Zhu et al., "The adsorption property and mechanism of phenyl/amine end-capped tetraaniline for alizarin red S," *Colloid & Polymer Science*, vol. 296, no. 11, pp. 1777–1786, 2018.

[54] W. M. Alghamdi and I. E. Mannoubi, "Investigation of seeds and peels of *Citrullus colocynthis* as efficient natural adsorbent for methylene blue dye," *Processes*, vol. 9, no. 8, p. 1279, 2021.

[55] M. A. Ahmad, M. A. Eusoff, P. O. Oladoye, K. A. Adegoke, and O. S. Bello, "Optimization and batch studies on adsorption of methylene blue dye using pomegranate fruit peel based adsorbent," *Chemical Data Collections*, vol. 32, article 100676, 2021.

[56] R. Ali, Z. Aslam, R. A. Shawabkeh, A. Asghar, and I. A. Hussein, "BET, FTIR, and Raman characterizations of activated carbon from waste oil fly ash," *Turkish Journal of Chemistry*, vol. 44, no. 2, pp. 279–295, 2020.

[57] I. Langmuir, "The adsorption of gases on plane surfaces of glass, mica and platinum," *Journal of the American Chemical Society*, vol. 40, no. 9, pp. 1361–1403, 1918.

[58] H. M. F. Freundlich, "Over the adsorption in solution," *The Journal of Physical Chemistry*, vol. 57, pp. 385–470, 1907.

[59] S. Lagergren, "About the theory of so-called adsorption of soluble substances," *KungligaSvenskaVetenskHandl.*, vol. 24, pp. 1–39, 1898.

[60] Y. S. Ho and G. MaKay, "Pseudo-second order model for sorption processes," *Process biochemistry*, vol. 34, no. 5, pp. 451–465, 1999.

[61] W. J. Weber and J. C. Morris, "Kinetics of adsorption on carbon from solution," *Journal of the sanitary engineering division*, vol. 89, no. 2, pp. 31–59, 1963.

[62] F. M. Machado, S. A. Carmalin, E. C. Lima et al., "Adsorption of alizarin red S dye by carbon nanotubes: an experimental and theoretical investigation," *Journal of Physical Chemistry C*, vol. 120, no. 32, pp. 18296–18306, 2016.

[63] R. Nodehi, H. Shayesteh, and S. Rahbar-Kelisham, "Fe_3O_4@-NiO core–shell magnetic nanoparticle for highly efficient removal of alizarin red S anionic dye," *International journal of Environmental Science and Technology*, vol. 19, no. 4, pp. 2899–2912, 2022.

[64] M. Roosta, M. Ghaedi, and M. Mohammadi, "Removal of alizarin red S by gold nanoparticles loaded on activated carbon combined with ultrasound device: optimization by experimental design methodology," *Powder Technology*, vol. 267, pp. 134–144, 2014.

[65] B. Wanassi, I. B. Hariz, C. M. Ghimbeu, C. Vaulot, and M. Jeguirim, "Green carbon composite-derived polymer resin and waste cotton fibers for the removal of alizarin red S dye," *Energies*, vol. 10, no. 9, p. 1321, 2017.

[66] P. K. Gautam, P. M. Shivapriya, S. Banerjee, A. K. Sahoo, and S. K. Samanta, "Biogenic fabrication of iron nanoadsorbents from mixed waste biomass for aqueous phase removal of alizarin red S and tartrazine: kinetics, isotherm, and thermodynamic investigation," *Environmental Progress & Sustainable Energy*, vol. 39, no. 2, 2020.

[67] E. Nasoudari, M. Ameri, M. Shams, V. Ghavami, and Z. Bonyadi, "The biosorption of alizarin red S by *Spirulina platensis*; process modelling, optimisation, kinetic and isotherm studies," *International Journal of Environmental Analytical Chemistry*, pp. 1–15, 2021.